

SUPPLEMENTAL MATERIAL

Jin et al., <https://doi.org/10.1085/jgp.201611684>

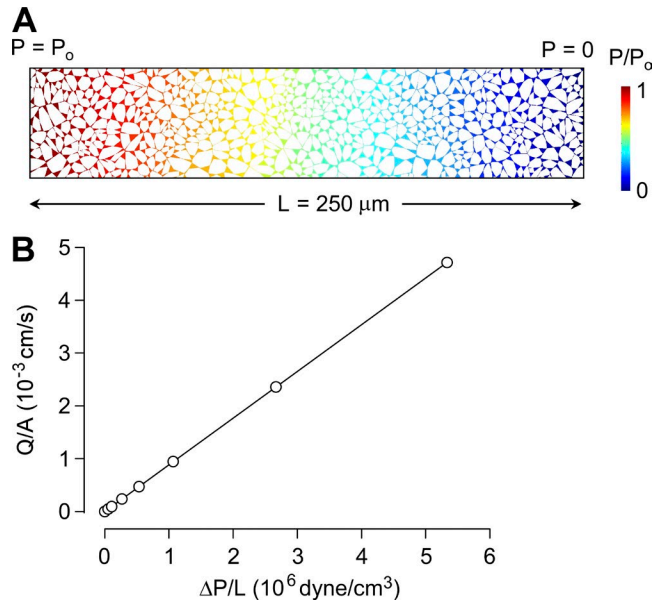


Figure S1. **Hydraulic conductance computation of the ECS model.** (A) Computational geometry with 250- $\mu\text{m}$  length and 50- $\mu\text{m}$  width, with pressure boundary condition at the inlet and symmetric boundary condition at the side walls. Pressure shown for  $\Delta P = 1$  mmHg for the same ECS model ( $\alpha = 0.2$ ) used in Fig. 2 C. (B) Relationship of computed volume flux to pressure difference. The hydraulic conductance ( $L_p$ ) was computed as  $0.9 \times 10^{-9} \text{ cm}^4/\text{dyne/s}$  using the equation  $Q/A = L_p \times \Delta P/L$ , where  $Q$  is total volume flux,  $A$  inlet area,  $\Delta P$  pressure difference, and  $L$  the length between the inlet and the outlet.

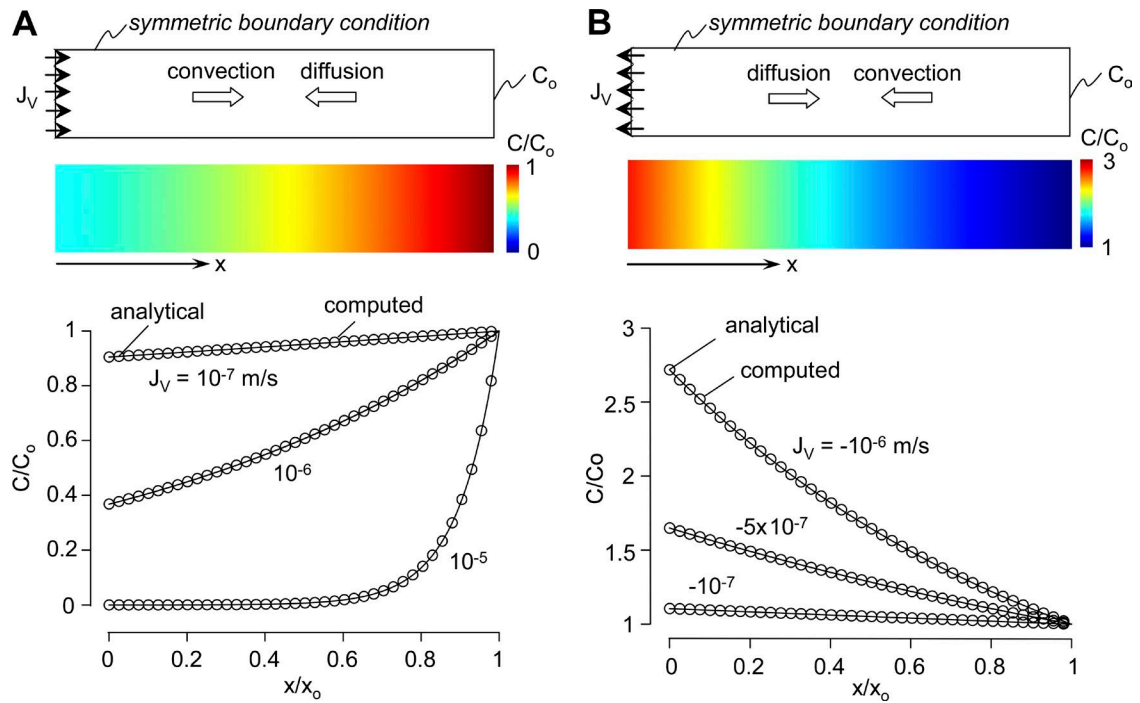


Figure S2. **Validation of advection–diffusion computation in one dimension in the absence of cell barriers.** (A and B) Advection–diffusion shown for inward (A) and outward (B) water flux  $J_v$  (top). The concentration at the boundary at  $x = x_0$  was fixed at  $C_0$ . The advection–diffusion equations for the steady state have an analytical solution:  $C(x) = C_0 \exp(J_v/D \times (x - x_0))$ , which agreed with computed results. The graphs show spatial concentration profile,  $C/C_0$ , determined by computation (circles) and analytical solution (curves) for the indicated  $J_v$ .

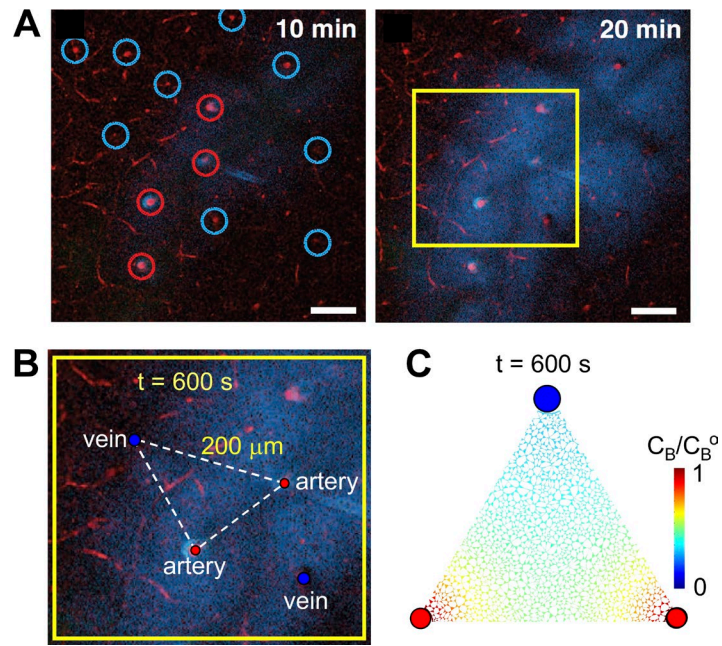


Figure S3. **Comparison of predictions of a diffusion-only ( $\Delta P = 0$ ) model with experimental data on solute accumulation in ECS.** (A) Experimental data taken from Fig. 2 of Iliff et al. (2012) with permission from the American Association for the Advancement of Science, showing accumulation of a 3-kD tracer from the paravascular space into the parenchyma. Red circles, arterioles; blue circles, venules. Bars,  $100 \mu\text{m}$ . (B) Dye accumulation in a region bounded by two arterioles and one venule (the yellow box shown in A), with fitted time constant  $\sim 600$  s. (C) Computed accumulation of solute B by diffusion alone shows similar filling time  $\sim 600$  s. Model parameters:  $P_f = 0.04$  cm/s,  $D = 2.2 \times 10^{-10}$  m<sup>2</sup>/s, and  $\alpha = 0.2$ .

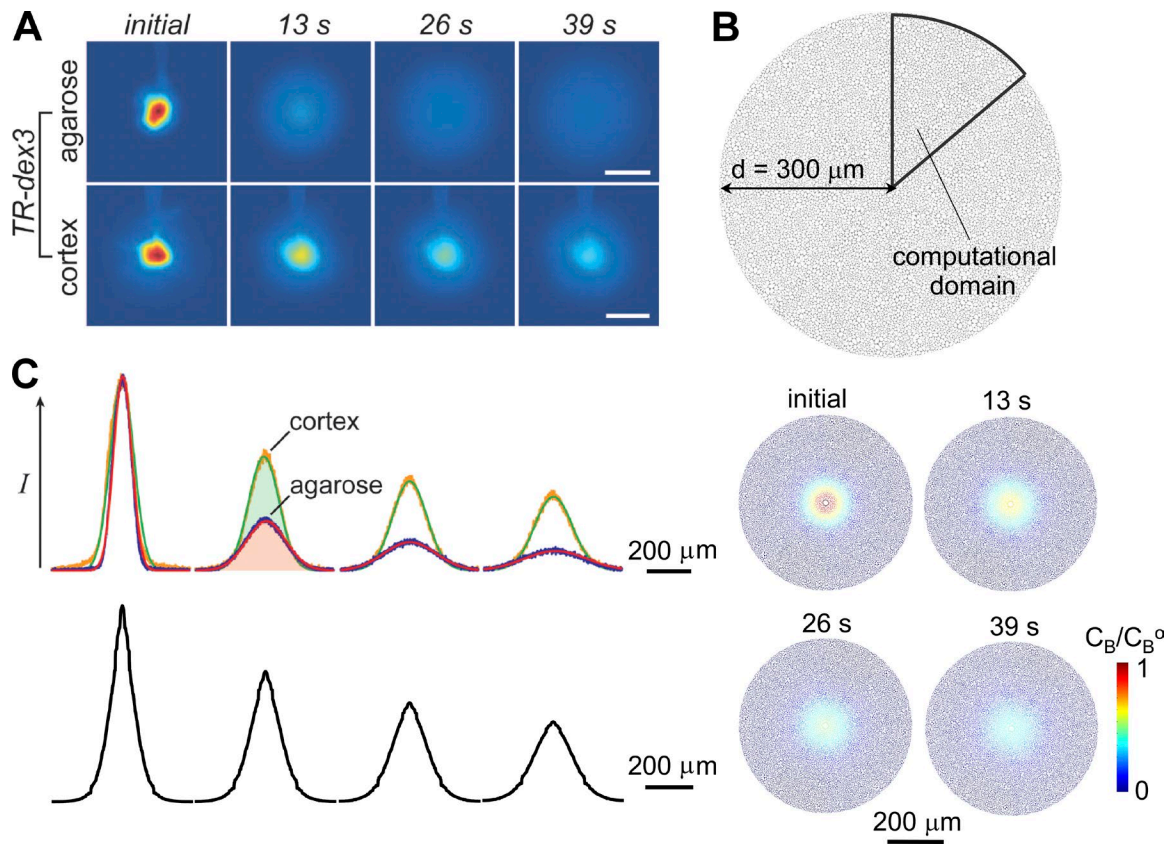


Figure S4. Comparison of predictions of a diffusion-only ( $\Delta P = 0$ ) model for the current ECS geometry with experimental data on diffusion of 3-kD Texas red-dextran in the ECS. (A) Experimental data taken from Fig. 3 of Thorne and Nicholson (2006), showing dispersal of Texas red fluorescence in agarose and brain cortex after 50- to 200-ms pressure ejection of the dye from a micropipette. The pseudocolored images show dye concentration at the indicated times. Bars, 200  $\mu\text{m}$ . (B) Computational modeling showing dispersal of fluorescence after pressure injection to recapitulate the experimental data. The same ECS geometry (60-nm median ECS width,  $\alpha = 0.2$ ) as in Fig. 2 was used for the computation. Symmetry allowed computation in the  $45^\circ$  domain shown. Fluorescent dye was injected through a 20- $\mu\text{m}$  diameter circle at the center at a pressure of 5 mmHg; injection was terminated after obtaining similar fluorescence dispersal as measured experimentally. The pseudocolored images show dye concentration at the indicated times, which is similar to the experimental data. (C) Comparison of experimental fluorescence profiles (top) and computed profiles (bottom) for  $D = 2.2 \times 10^{-10} \text{ m}^2/\text{s}$  with  $\alpha = 0.2$  for the indicated times.

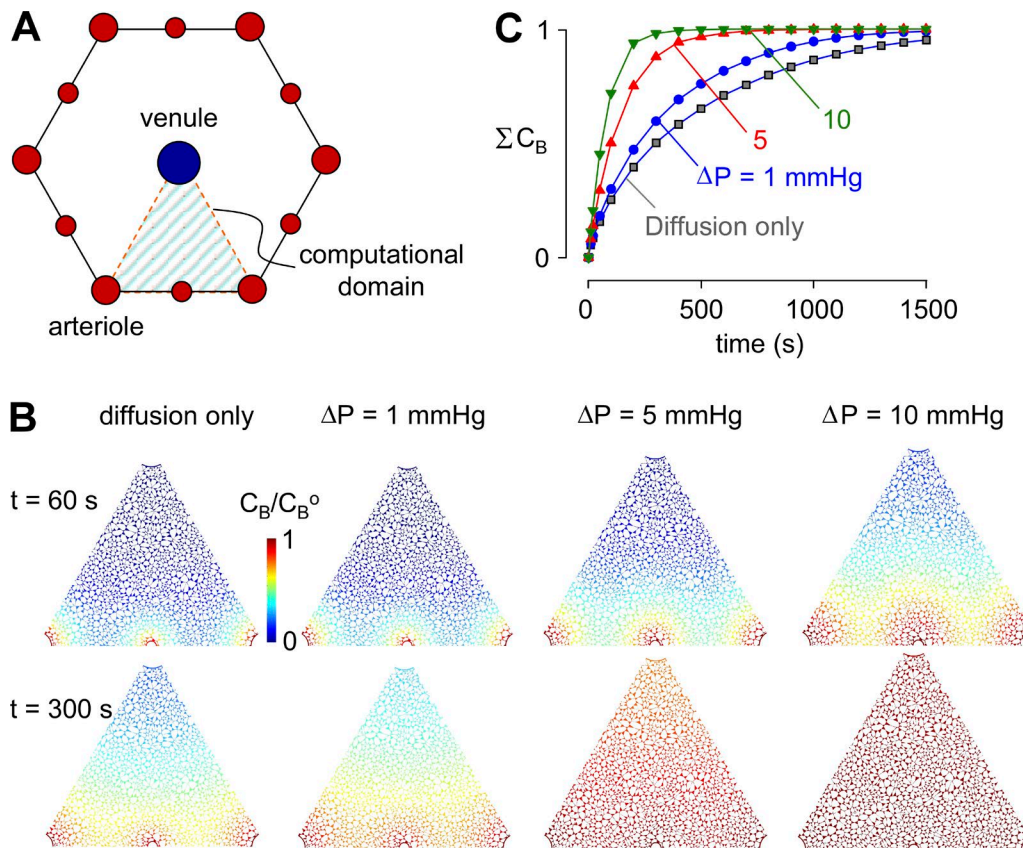


Figure S5. **Convective fluid movement from para-arterial to paravenous spaces in brain ECS with an altered geometry of three arterioles and one venule.** (A, left) Hexagonal spatial arrangement of arterioles and venule showing triangular computational domain (right) with three arterioles and one venule. (B) Pseudocolored images showing tracer solute accumulation in ECS after a step increase in para-arterial tracer concentration for para-arterial to paravenous pressure differences  $\Delta P$  of 0 (diffusion alone) or 1, 5, and 10 mmHg. Parameters:  $P_f = 0.04$  cm/s and  $D = 10^{-10}$  m<sup>2</sup>/s. (C) Kinetics of tracer solute accumulation in ECS for the indicated  $\Delta P$ .

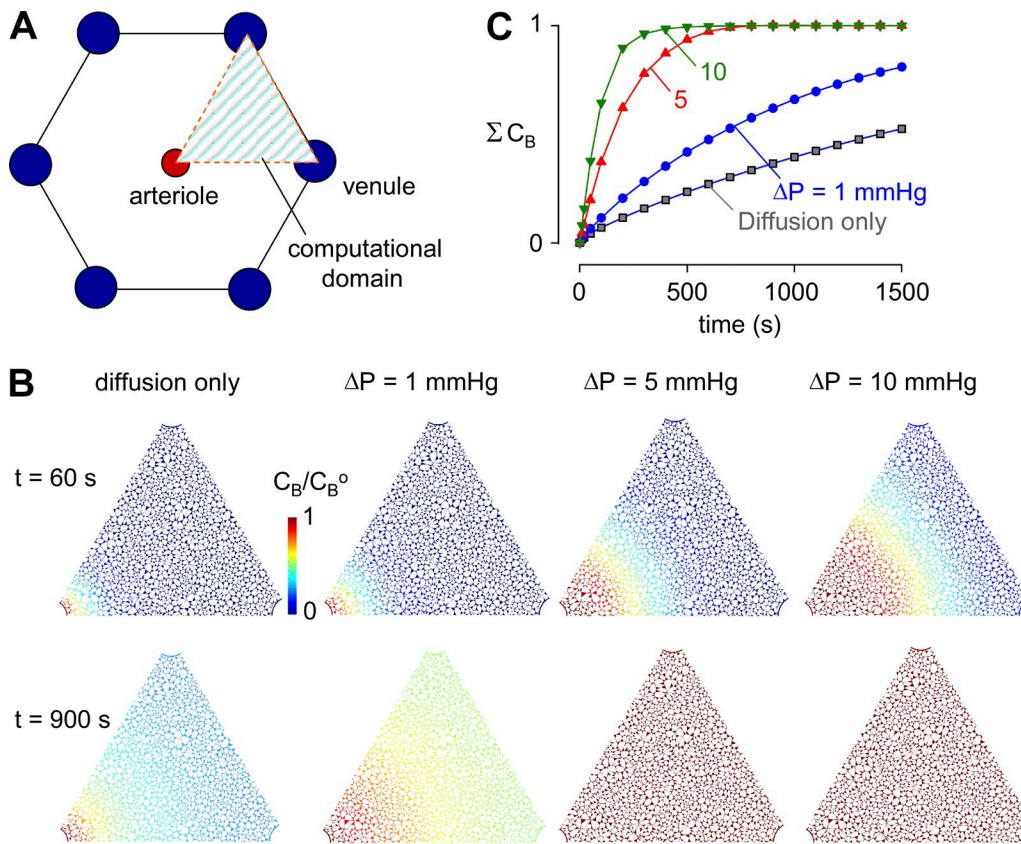


Figure S6. **Convective fluid movement from para-arterial to paravenous spaces in brain ECS with altered geometry.** (A, left) Hexagonal spatial arrangement of arterioles and venules (in rodent brain parenchyma) showing triangular computational domain (right) with one arteriole and two venules. (B) Pseudocolored images showing tracer solute accumulation in ECS after a step increase in para-arterial tracer concentration for para-arterial to paravenous pressure differences  $\Delta P$  of 0 (diffusion alone) or 1, 5, and 10 mmHg. Parameters:  $P_f = 0.04$  cm/s and  $D = 10^{-10}$  m<sup>2</sup>/s. (C) Kinetics of tracer solute accumulation in ECS for the indicated  $\Delta P$ .

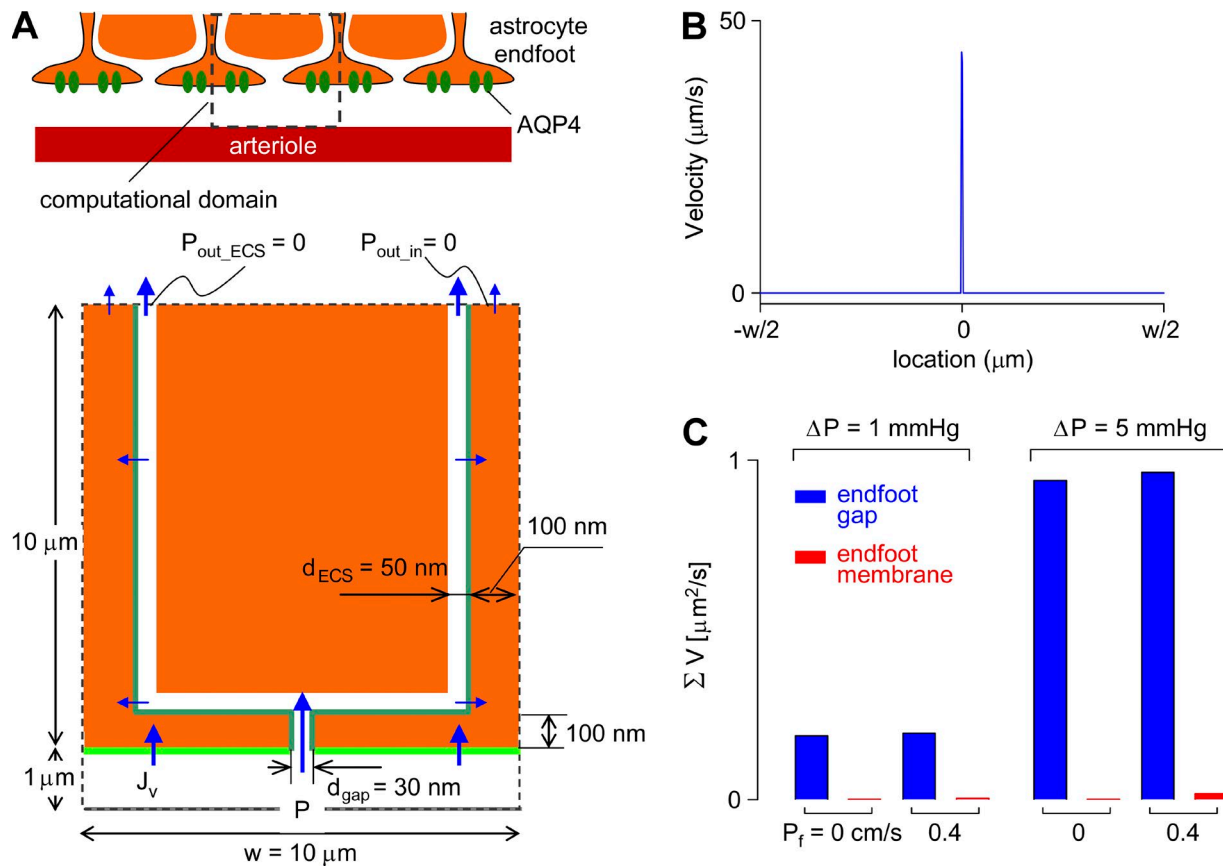


Figure S7. **Advective fluid movement through versus around astrocyte endfeet.** (A) Diagram of water movement through and around astrocyte endfeet. Symmetry in the modeled geometry (top) allowed the indicated computation domain (bottom). For computations, the astrocyte endfoot water permeability was  $0.4 \text{ cm/s}$  (modeling physiologically high AQP4 density), and that of the cell membrane was  $0.04 \text{ cm/s}$ . Cells between astrocytes (such as neurons) were taken as impermeable. The para-arterial space boundary was modeled as a constant pressure boundary condition ( $P = 1$  or  $5 \text{ mmHg}$ ). Fluid transport through the endfoot membrane was modeled as described in Materials and methods. (B) Velocity profile at the astrocyte endfoot membrane and gap. (C) Area-integrated velocity at the astrocyte endfoot membrane and gap for the indicated pressure difference ( $\Delta P$ ) and water permeability ( $P_f$ ).

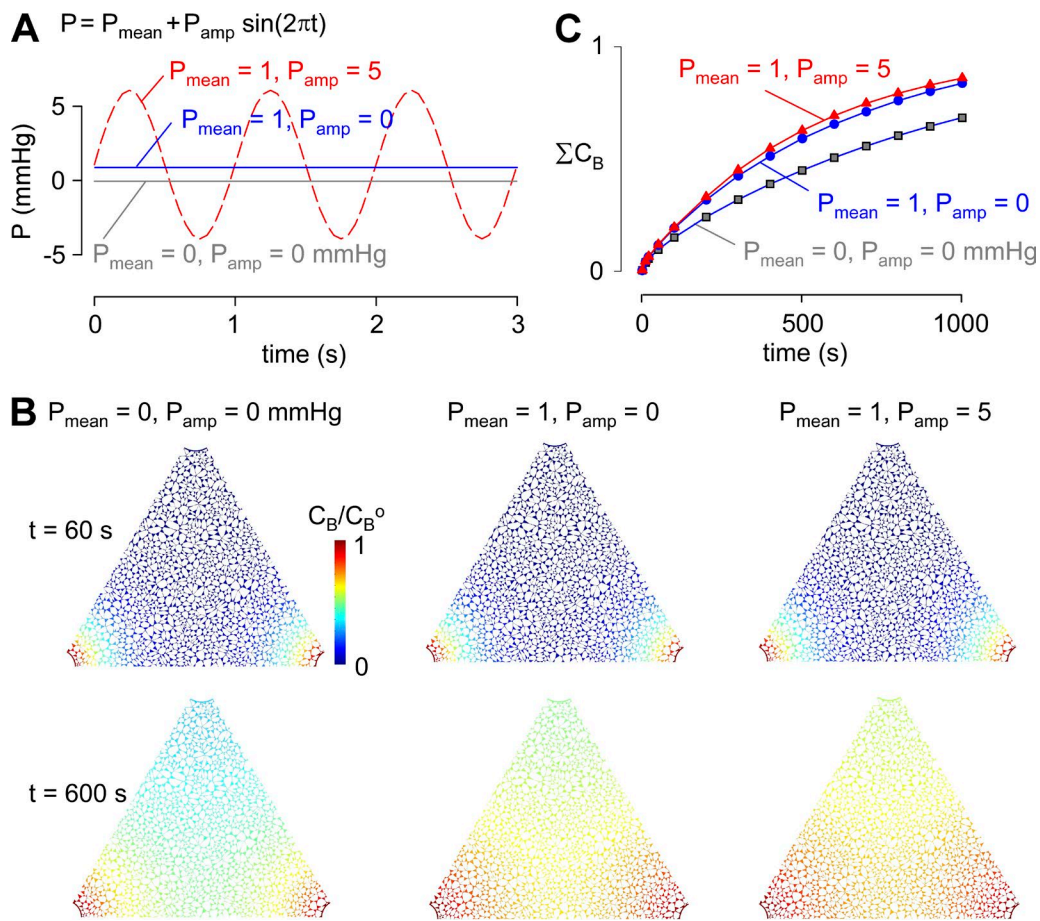
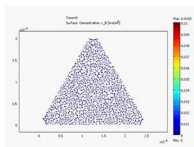
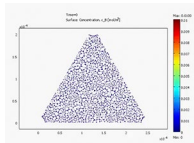


Figure S8. **Influence of baseline mean pulsatile pressure in the para-arterial space on solute movement in brain ECS.** (A) Para-arterial pressure waveform of mean pressure  $P_{\text{mean}}$ , amplitude  $P_{\text{amp}}$ , and frequency 1 Hz. (B) Pseudocolored images showing tracer solute accumulation in the ECS for the indicated  $P_{\text{mean}}$  and  $P_{\text{amp}}$ . Parameters:  $P_f = 0.04$  cm/s,  $D = 10^{-10}$  m<sup>2</sup>/s, and  $\alpha = 0.2$ . (C) Kinetics of tracer solute accumulation in ECS for the indicated  $P_{\text{mean}}$  and  $P_{\text{amp}}$ .

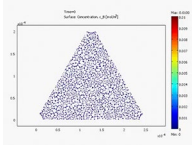


Video 1. **Accumulation of solute B in the ECS for the absence of a pressure difference ( $\Delta P = 0$ , diffusion alone).** Model parameters:  $P_f = 0.04$  cm/s,  $D = 10^{-10}$  m<sup>2</sup>/s, and  $\alpha = 0.2$ .



Video 2. **Accumulation of solute B in the ECS for pressure difference  $\Delta P = 1$  mmHg.** Model parameters:  $P_f = 0.04$  cm/s,  $D = 10^{-10}$  m<sup>2</sup>/s, and  $\alpha = 0.2$ .





Video 3. **Accumulation of solute B in the ECS for pressure difference  $\Delta P = 10$  mmHg.** Model parameters:  $P_i = 0.04$  cm/s,  $D = 10^{-10}$  m<sup>2</sup>/s, and  $\alpha = 0.2$ .

## REFERENCES

- Illiff, J.J., M. Wang, Y. Liao, B.A. Plogg, W. Peng, G.A. Gundersen, H. Benveniste, G.E. Vates, R. Deane, S.A. Goldman, et al. 2012. A paravascular pathway facilitates CSF flow through the brain parenchyma and the clearance of interstitial solutes, including amyloid  $\beta$ . *Sci. Transl. Med.* 4:147ra111. <http://dx.doi.org/10.1126/scitranslmed.3003748>
- Thorne, R.G., and C. Nicholson. 2006. In vivo diffusion analysis with quantum dots and dextrans predicts the width of brain extracellular space. *Proc. Natl. Acad. Sci. USA.* 103:5567–5572. <http://dx.doi.org/10.1073/pnas.0509425103>